

$\frac{19}{2}^-$ g factor in ^{39}K using a transient field-fusion reaction technique

A. A. Pakou

*Department of Physics, The University of Ioannina, Ioannina, Greece
and Dipartimento di Fisica dell' Università, Padova and Istituto Nazionale di Fisica Nucleare, Padova, Italy*

F. Brandolini, D. Bazzacco, P. Pavan, C. Rossi-Alvarez, and E. Maglione

Dipartimento di Fisica dell' Università, Padova and Istituto Nazionale di Fisica Nucleare, Padova, Italy

M. DePoli and R. Ribas*

Istituto Nazionale di Fisica Nucleare, Laboratori Nazionali di Legnaro, Legnaro, Italy

(Received 10 July 1991)

The magnetic moment of the $\frac{19}{2}^-$ state in ^{39}K has been measured by the transient field technique. The state was excited by the inverse reaction $^{12}\text{C}(^{32}\text{S}, p\alpha)^{39}\text{K}$ and the recoil nucleus traversed a thin Gd foil. Its absolute g factor, $g=0.35(3)$, was obtained by an internal calibration, which makes use of the magnetic moment of the $\frac{15}{2}^+$ state in ^{41}Ca also excited in the same reaction. A mean g factor for the states 3^- , 5^- in ^{36}Ar , $g=0.52(6)$, determined in a simultaneous measurement is consistent with the self-conjugate nature of the nucleus, giving further support to the validity of the field calibration. The experimental result agrees with shell-model predictions.

PACS number(s): 21.10.Ky, 27.40.+z

I. INTRODUCTION

In the last few years the transient field technique has proved a valuable tool for the measurement of magnetic moments of short-lived states. The excitation process most widely used for accurate determination of moments of short-lived states is, by far, Coulomb excitation. However, the states accessible through this process have recently been almost exhausted. Thus a new technique for excitation of high spin states is being sought, and as such, the heavy-ion fusion-evaporation reaction of the type $(\text{HI}, \alpha p n \gamma)$ seems the most promising.

The highly excited states formed through such reactions, after particle emission, first decay down to the yrast region via complex paths of "statistical" transitions that carry off energy but little angular momentum, such as $E1$ decays, or of "yrastlike" transitions which remove angular momentum along the yrast line through either collective rotational or single-particle transitions.

Subsequently, after the nucleus has cooled down sufficiently, the decay condenses into a few pathways in the yrast region. These last decays stand out in the spectrum and can be resolved by γ -ray spectroscopy methods accessible today. The application of the transient field technique to such states, for the measurement of magnetic moments, is however hindered by the unknown history of their formation, the knowledge of which is vital.

In this context, to make unambiguous measurements,

either additional handles to the usual transient field method must be invoked or nuclei and reactions with sufficiently simple feeding patterns must be selected. In the heavy mass region a combination of transient fields and plunger measurements are at an exploratory stage in this and other laboratories. Two recent measurements [1,2] have already been reported. In the mass region $A=70$, a few attempts with the conventional transient field method have been limited either to mean g factors [3] or have yielded results [4,5] valid under certain feeding assumptions.

In the present work, we report g -factor measurements in the $A=40$ region, through the conventional transient field method [6] and by utilizing, as an excitation process, the inverse reaction $^{32}\text{S} + ^{12}\text{C}$, which leads to the residual nucleus via simple patterns. The motivation for such measurements stems from the following reasons.

(a) The well-known γ -ray spectroscopy in the region concerning energy levels, spins, and lifetimes through experiments with both light- and heavy-ion beams [7-14]. In particular, ^{39}K was carefully studied previously [13] via a fusion reaction leading to the same compound nucleus as in the present work. The $\frac{19}{2}^-$ was the highest spin state reached with observable intensity. A level scheme is shown in Fig. 1. Lifetime assignments are from Nolan *et al.* [14], and references therein.

(b) Results of CASCADE [15] statistical calculations show that the residual nucleus is left at a rather low excitation energy of 12 MeV. In this energy region present shell-model calculations, shown in Fig. 1, predict a rather low-energy level density which results only in a discrete γ -ray pattern.

(c) Both nuclei ^{41}Ca and ^{36}Ar are populated simultane-

*Present Address: University of São Paulo, Institute of Physics, Pelletron Laboratory, São Paulo, Brazil.

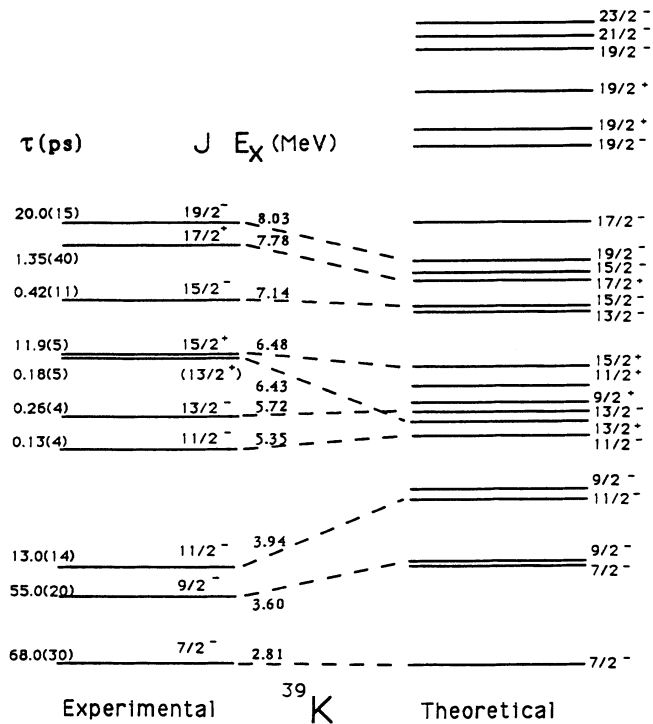


FIG. 1. States in ^{39}K , strongly populated in fusion reaction, compared with shell-model calculations described in the text. For reasons of simplicity only the two lowest states for given spin and parity ($J = \frac{9}{2}$ to $\frac{23}{2}$) are reported.

ously with ^{39}K in the same reaction. The well-known magnetic moment [16,17] of the $\frac{15}{2}^+$ state in ^{41}Ca which has a rather long meanlife ($\tau = 4500$ ps), but is nevertheless still amenable to a measurement via the transient field technique, and allows for an unambiguous calibration of the field. In the same context, the g factors of the ^{36}Ar nucleus are reliably predicted [18] and the predictions are supported by experimental data.

(d) Existing shell-model calculations describe the $\frac{19}{2}^-$ state of ^{39}K as an $^{36}\text{Ar}(0^+) \oplus f_{7/2}^3$ state. If this description is adequate, a g factor similar to that of ^{43}Sc , $g = 0.328(7)$ (Ref. [19]), can be expected. On the other hand, contributions of the $f_{5/2}$ orbit and configuration mixing of the ^{36}Ar core may likely change this value.

Finally, we have to point out that ^{39}K is the lightest nucleus for which a fusion reaction has been used to measure the g factor of an individual high spin state. The transient field technique, with a thin gadolinium foil as a ferromagnet, has proved to be the most favorable method for measuring magnetic moments of short-lived states in that mass region, since despite the low Z of the nuclei involved, the observed strength of the field is high. The ion implantation perturbed angular distribution (IMPAD) technique cannot be applied in the specific case of ^{39}K , because the static field is small and affected by radiation damage [20], while a recoil in gas technique applied previously [21] to measure the moments of lower states in nuclei in this mass region is less sensitive for high spin states.

II. EXPERIMENTAL DETAILS

Since the thin-foil transient field method has been described by Benczer-Koller, Hass, and Sak [6] and the details of our setup have been outlined in previous publications [22,23], we will present here only the features particular to this work.

The inverse reaction $^{12}\text{C}(^{32}\text{S},\alpha p)^{39}\text{K}$ was used to populate the states of interest at a beam energy of 115 MeV supplied by the 17 MV XTU tandem accelerator of LNL (Laboratori Nazionali di Legnaro). In the same experiment, states in ^{41}Ca and ^{36}Ar were also populated and studied under identical conditions.

The experiment was designed to observe the integral of the γ -ray angular correlation pattern, as the nuclei are moving through a polarized ferromagnetic layer.

The target foil was a five-layer sandwich. A 5 mg/cm^2 gadolinium foil was separated from the $500 \mu\text{g/cm}^2$ carbon and the 25 mg/cm^2 silver backing, by two indium layers of $300 \mu\text{g/cm}^2$ each. Initially the indium layers, used to ensure good adherence of the target and backing materials, were evaporated on the front and back faces of the gadolinium foil. Subsequently the carbon layer and silver backing foil were pressed on the front and back faces of the three layer In-Gd-In foil. The thickness of the carbon target plus the indium layer allowed a time of 100 fs for any fast feeding to take place before the nuclei enter into the ferromagnet. The thick silver backing foil, used to stop the beam and recoiling ions, acted also as a good thermal dissipator.

The gadolinium foil, supplied by Goodfellow Metals, was first rolled down to the desired thickness, annealed at 600°C for a few minutes in a vacuum of 10^{-1} bar and then cleaned with glow discharge. Subsequently, it was tested for magnetization in a double magnetometer and found to be 79% magnetized ($6e^-/\text{atom}$). The thickness of the foil was measured both with an Am α source and by estimating its weight and surface area.

The target sandwich was clamped between the poles of an electromagnet and was polarized in a field of 0.027 T which was reversed periodically. Due to the low applied field, sufficient however for polarizing the gadolinium foil, beam bending effects were negligible and corrections in the rotations of long-lived states were kept at a minimum. The temperature of the target was maintained at 88 K by cooling [22] with liquid nitrogen.

A second target consisting of a self-supporting carbon foil, $500 \mu\text{g/cm}^2$ thick, was used in a separate experiment to determine, via the Doppler effect, the mean ion exit velocity from the foil and thus the mean ion recoil entrance velocity into the gadolinium foil used for the g -factor run. Mean ion recoil energies determined in this way, and corrected for energy loss in the indium separator, were $E_{\text{in}} = 58, 58, 65 \text{ MeV}$ for ^{39}K , ^{41}Ca , ^{36}Ar , respectively.

Prompt γ rays from the various reaction channels were detected in four Compton suppressed, 25% efficiency, Ge detectors from the LNL facility. The detectors were located at $\pm 65^\circ$, $\pm 115^\circ$ with respect to the beam, and at a distance of 17 cm from the target.

The slope of the angular distribution at the angle of interest was measured directly several times during the

course of the experiment. For this purpose the detectors were moved automatically every 20 min by $\pm 3^\circ$ from their original position. Furthermore, an actual angular distribution was measured to corroborate the slope measurements. That measurement was carried out by one detector which was placed successively at $100^\circ, 115^\circ, 137^\circ, 145^\circ$, the only technically accessible positions, while two other detectors were set at fixed positions and served as monitors.

III. SPECTRA ANALYSIS

Two typical Compton suppressed γ spectra are shown in Figs. 2(a) and 2(b). Both spectra were collected with detector 1, set at an angle of 65° with respect to the beam. In order to facilitate the analysis and simultaneously to accept as high energies as possible, one spectrum was

recorded within the range of 0 to 1400 keV [Fig. 2(a)], while the other was observed between 1400 and 4400 keV [Fig. 2(b)]. In Figs. 2(a) and 2(b) strong γ rays are numbered and identified in Table I. As seen, in these spectra, the following reactions are observed: $2p + {}^{42}\text{Ca}$, $2pn + {}^{41}\text{Ca}$, $3p + {}^{41}\text{K}$, $\alpha 2p + {}^{38}\text{Ar}$, and $2\alpha + {}^{36}\text{Ar}$, in addition to the $\alpha p + {}^{39}\text{K}$ where our main interest lies.

The γ spectra obtained after imposing the Compton rejection restriction, show very low background. As an example, considering the 886 keV line, the peak to background ratio was 2.6 against a ratio of 0.8 in single spectra.

The "effect" spectra observed for the precession measurements were sufficiently clean so that the analysis was not affected by spurious line shapes due to Doppler shift effects. However, the analysis of the "slope" and "angular correlation" spectra was sometimes difficult and the results had to corroborate each other. In particular, for the 886 keV peak of ${}^{39}\text{K}$ an additional problem seemed initially to arise from a small unresolved peak at 889 keV (Fig. 3). This peak, identified as belonging to ${}^{46}\text{Ti}$, is pro-

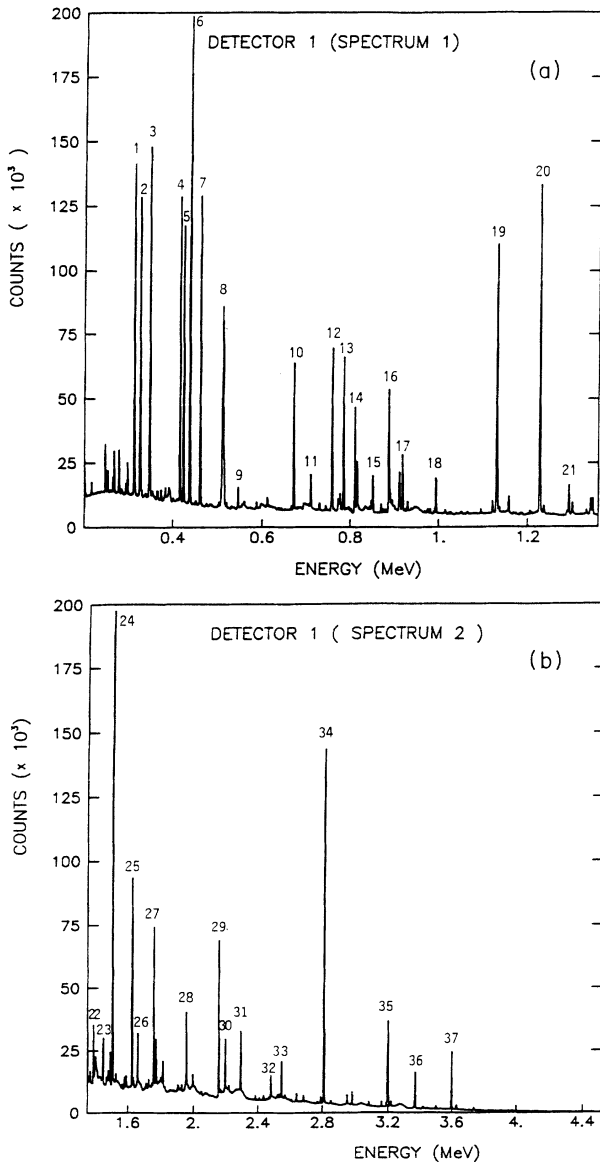


FIG. 2. γ spectra collected with CS Ge (Compton suppressed Ge) detectors. (a) Range 1–1400 keV; (b) range 1400–4400 keV.

TABLE I. Identification of γ -rays shown in Figs. 1 and 2.

Spectrum	E_γ (keV)	$J_i \rightarrow J_f$	Nucleus
2	347	$\frac{11}{2}^- \rightarrow \frac{9}{2}^-$	${}^{39}\text{K}$
6	437	$6^+ \rightarrow 4^+$	${}^{42}\text{Ca}$
7	460	$\frac{15}{2}^+ \rightarrow \frac{11}{2}^+$	${}^{41}\text{Ca}$
8	511	$e^+ e^-$	
11	708	$\frac{19}{2}^- \rightarrow \frac{15}{2}^-$	${}^{41}\text{K}$
12	757	$\frac{15}{2}^+ \rightarrow \frac{13}{2}^-$	${}^{39}\text{K}$
13	783	$\frac{9}{2}^- \rightarrow \frac{7}{2}^-$	${}^{39}\text{K}$
14	810	$9^- \rightarrow 7^-$	${}^{42}\text{Ca}$
14	814	$(8, 10)^- \rightarrow 9^-$	${}^{42}\text{Ca}$
15	850	$\frac{11}{2}^+ \rightarrow \frac{7}{2}^+$	${}^{41}\text{K}$
16	887	$\frac{19}{2}^- \rightarrow \frac{15}{2}^-$	${}^{39}\text{K}$
17	910	$5^- \rightarrow 6^+$	${}^{42}\text{Ca}$
17	918	$8^- \rightarrow 6^-$	${}^{42}\text{Ca}$
18	993	$5^- \rightarrow 3^-$	${}^{36}\text{Ar}$
19	1130	$\frac{11}{2}^- \rightarrow \frac{7}{2}^-$	${}^{39}\text{K}$
20	1228	$4^+ \rightarrow 2^+$	${}^{42}\text{Ca}$
21	1300	$\frac{17}{2}^+ \rightarrow \frac{15}{2}^-$	${}^{39}\text{K}$
22	1410	$\frac{11}{2}^- \rightarrow \frac{11}{2}^-$	${}^{39}\text{K}$
23	1468	$\frac{11}{2}^- \rightarrow \frac{7}{2}^-$	${}^{41}\text{K}$
24	1525	$2^+ \rightarrow 0^+$	${}^{42}\text{Ca}$
25	1644	$7^- \rightarrow 5^-$	${}^{42}\text{Ca}$
26	1677	$\frac{7}{2}^+ \rightarrow \frac{3}{2}^+$	${}^{41}\text{K}$
27	1774	$\frac{13}{2}^- \rightarrow \frac{11}{2}^-$	${}^{39}\text{K}$
28	1970	$2^+ \rightarrow 0^+$	${}^{36}\text{Ar}$
29	2168	$2^+ \rightarrow 0^+$	${}^{38}\text{Ar}$
30	2208	$3^- \rightarrow 2^+$	${}^{36}\text{Ar}$
31	2302	$6^- \rightarrow 6^+$	${}^{42}\text{Ca}$
32	2490	$\frac{13}{2}^+ \rightarrow \frac{11}{2}^-$	${}^{39}\text{K}$
33	2555	$7^- \rightarrow 6^+$	${}^{42}\text{Ca}$
34	2814	$\frac{7}{2}^- \rightarrow \frac{3}{2}^+$	${}^{39}\text{K}$
35	3197	$\frac{15}{2}^- \rightarrow \frac{11}{2}^-$	${}^{39}\text{K}$
35	3200	$\frac{9}{2}^+ \rightarrow \frac{7}{2}^-$	${}^{41}\text{Ca}$
36	3369	$\frac{11}{2}^+ \rightarrow \frac{7}{2}^-$	${}^{41}\text{Ca}$
37	3597	$\frac{9}{2}^- \rightarrow \frac{3}{2}^+$	${}^{39}\text{K}$

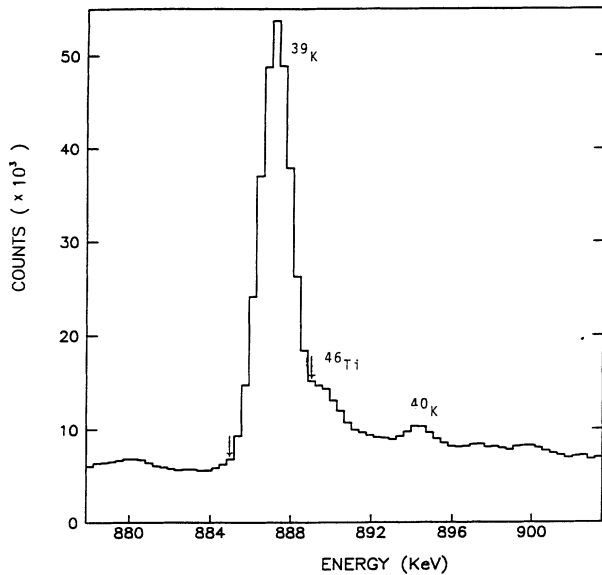


FIG. 3. Details of the 886 keV peak.

duced via the reaction $^{16}\text{O}(^{32}\text{S},2p)^{46}\text{Ti}$, due to oxygen contamination of the target. However, the precession effects obtained by integrating the 886 keV peak intensity, either by summing the counts between the arrows marked in Fig. 3 or by fitting a double or multiple Gaussian to the whole line shape shown in the figure, were identical. This result was mainly attributed to the fact that the contribution of the 889 keV ^{46}Ti peak to the 886 keV ^{39}K peak was estimated to be as small as $(4 \pm 0.2)\%$. Thus no correction was necessary in the analysis of the 886 keV peak of ^{39}K .

IV. REDUCTION OF DATA AND RESULTS

Our data analysis is based on the observation that the $\frac{19}{2}^-$ state in ^{39}K is directly populated. In more detail, any discrete or continuum feeding was excluded for the following reasons.

Discrete feeding: As already stated, results of CASADE [15] calculations show that after the evaporation of the particles the residual nucleus is left at an excitation energy of about 12 MeV. As it is evident from Fig. 1, where a calculated level scheme is presented, the level density in this energy region is low and would give rise only to discrete γ rays. However, no such γ -rays depopulating states higher than the $\frac{19}{2}^-$ state were identified in our spectra although states like the $\frac{21}{2}, \frac{23}{2}$ are highly favored by the evaporation of charged particles. Moreover, no such lines were reported previously [13] in the reaction $^{28}\text{Si}(^{16}\text{O},\alpha p)^{39}\text{K}$ leading to the same compound nucleus where γ - γ coincidences were performed. Specifically in the energy range of 200 to 4000 keV no lines in coincidence with the 886 keV line, other than those seen in the decay of the $\frac{19}{2}^-$ state, were observed up to a limit of $\approx 5\%$.

Continuum feeding: The continuum feeding, if any, was reported [24] to be fast in this mass region and less than 200 fs. If we consider that the recoil nucleus spends

an average of 100 fs in the C and In layers before entering the gadolinium foil and that the transit time in Gd is about 500 fs, such feeding will be only a small fraction of the total yield and thus be negligible. On the other hand, a direct proof of that conclusion was sought in our spectra. In Fig. 4, a partial γ -ray spectrum is displayed, where the 1410 keV line is shown to have a fully Doppler-shifted component in accordance with its short lifetime of 0.13(4) ps and condition of direct feeding. This line depopulates the 5.35 MeV state via a $\frac{11}{2}^- \rightarrow \frac{11}{2}^-$ transition (Fig. 5). Last, we refer to another previous

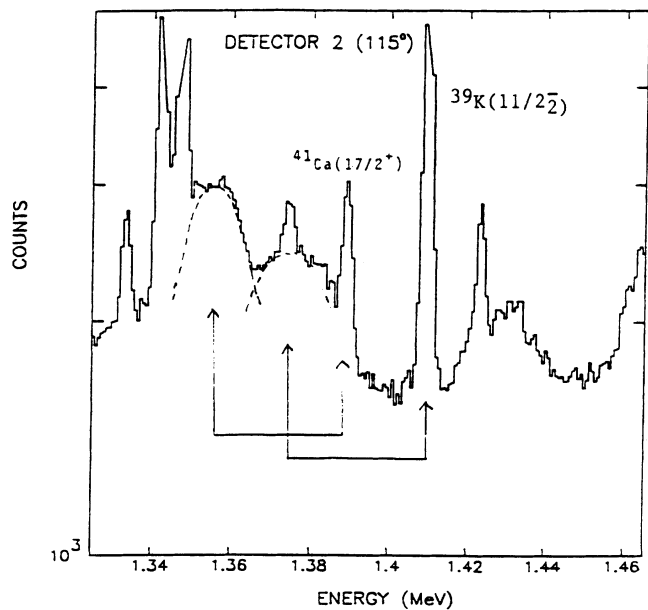
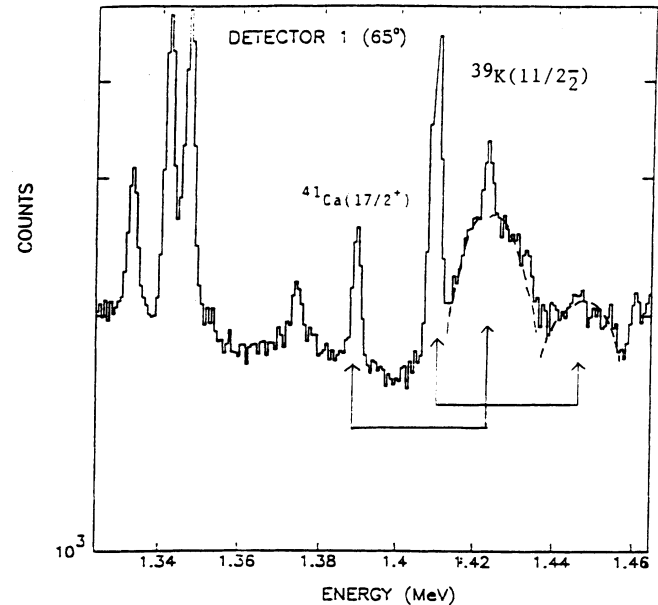


FIG. 4. Details of the decay of the $\left[\frac{11}{2}\right]_2$ state in ^{39}K via the 1410 keV line and of the $\frac{17}{2}^+$ state in ^{41}Ca via the 1389 keV one. In both cases full Doppler shift is observed, indicating a fast feeding.

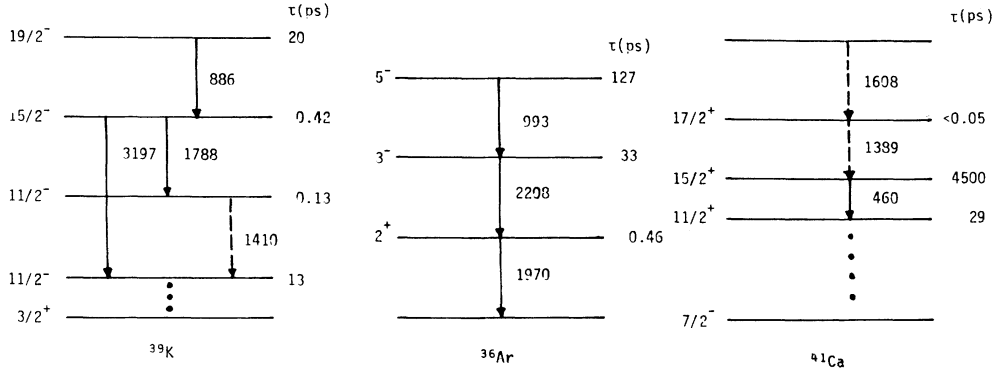


FIG. 5. Partial decay schemes of ^{39}K , ^{41}Ca , ^{36}Ar (Refs. [13,34,35]) concerning decays studied in this work.

publication [25] where, via a reaction similar to ours, entry states were determined. It was concluded, that the energy curve of the specific reaction exhibited very little correlation between excitation energy and spin, while it was terminated at an angular momentum of about $9\hbar$ to $10\hbar$.

Summarizing, we consider that the $\frac{19}{2}^-$ state in ^{39}K is populated directly and not fed by any other path. Thus we will proceed in the reduction of our data accordingly to the conventional transient field method.

The nuclear precessions of the γ -ray distribution, under reversal of the external magnetic field, were deduced by forming a double ratio of counting rates, N , for adjacent pairs of detectors:

$$\rho_{ij} = \frac{N_i(\uparrow) N_j(\downarrow)}{N_i(\downarrow) N_j(\uparrow)}, \quad \rho = (\rho_{12}\rho_{34})^{1/2}. \quad (1)$$

Then the rotation $\Delta\theta$ was obtained from the measured effect:

$$\varepsilon = \frac{\sqrt{\rho} - 1}{\sqrt{\rho} + 1} \quad (2)$$

and the slope $S(\theta)$ of the distribution:

$$\Delta\theta = \frac{\varepsilon}{S(\theta)}. \quad (3)$$

The magnetic moment of the $\frac{19}{2}^-$ state of ^{39}K was measured by observing the precession of the angular correlations of three γ -ray transitions (Fig. 5): the $\frac{19}{2}^- \rightarrow \frac{15}{2}^-$, 886 keV line, depopulating the long-lived $\tau = 20$ ps $\frac{19}{2}^-$ state, and the 1788 and 3197 keV lines depopulating the short-lived $\tau = 0.42$ ps, $\frac{15}{2}^-$, state. As this level is only fed by the 886 keV transition, the effect observed for the 1788 and 3197 keV transitions represents the precession of the initial $\frac{19}{2}^-$ state. The three precessions measured are in very good agreement. Thus their mean value is finally adopted as the rotation of the $\frac{19}{2}^-$ state. The results are summarized in Table II.

In the same table, information concerning calibration lines of the ^{41}Ca and ^{36}Ar nuclei is also presented.

The rotation of the $\frac{15}{2}^+$ state of ^{41}Ca , deduced from the 460 keV line ($\frac{15}{2}^+ \rightarrow \frac{11}{2}^+$ transition—Fig. 5), was not corrected for any continuum or discrete feeding for the same reasons as those presented for the $\frac{19}{2}^-$ state in ^{39}K . In more detail, only one line at 1389 keV is observed in our spectra contributing 30% of the yield of the 460 keV line. However, this line depopulates the $\frac{17}{2}^+$ state, which

TABLE II. Summary of experimental precession angles and slopes for states studied in the $^{12}\text{C} + ^{40}\text{Ca}$ reaction.

Nucleus	$J_i^\pi \rightarrow J_f^\pi$	E_γ (MeV)	$(v/v_0)_{\text{in}}$	$(V/v_0)_{\text{out}}$	τ^a (ps)	Slope (65°)	$-\Delta\theta$ (mrad)	g adopted
^{39}K	$\frac{19}{2}^- \rightarrow \frac{15}{2}^-$	0.886	7.7	3.8	20.0(15)	0.62(3)	13.38(94)	0.35(3)
	$\frac{15}{2}^- \rightarrow \frac{11}{2}^-$	3.197			0.42(11)	0.69(10)	13.89(370)	
	$\frac{15}{2}^- \rightarrow \frac{11}{2}^-$	1.788			0.42(11)	0.72(8)	14.65 (285)	
						$\Delta\theta_{\text{mean}} = 13.53(87)$		
^{41}Ca	$\frac{15}{2}^+ \rightarrow \frac{11}{2}^+$	0.461	7.6	3.6	4500(200)	0.63(2)	11.5(7) ^b	0.296(17) ^c
^{36}Ar	$5^- \rightarrow 3^-$	0.993	8.5	4.9	127(5)	0.56(6)	19.8(29)	0.52(6)
	$3^- \rightarrow 2^+$	2.208			3.3(4)	0.31(6)	24.3(64)	
	$2^+ \rightarrow 0^+$	1.970			0.46(4)	0.48(5)	19.7(31)	
						$\Delta\theta_{\text{mean}} + 20.2(20)$		

^aReferences [13,14,26].

^bCorrected by a factor of 1.7 ± 0.17 mrad due to the external field $B = 0.0270 \pm 0.0020$ T: $\Delta\theta = Bg(\mu/\hbar)\tau$, $\tau = 4500 \pm 200$ ps, $g = 0.296 \pm 0.017$.

^cCalibration point, Refs. [16,17].

was found previously in a prompt reaction [26] to be particularly short lived, $\tau \leq 50$ fs, and thus does not experience a measurable transient field rotation. On the other hand, the $\frac{17}{2}^+$ state itself is fed by a 1608 keV line depopulating a 6826 keV level of unknown spin and lifetime, but to an extent of at most only 6% (present data). Presumably due to that discrete or either continuum feeding, a longer effective lifetime of $\tau \leq 500$ fs was attributed to the $\frac{17}{2}^+$ level in a previous fusion reaction study [27]. This limit is reduced to 200 fs in the present experiment (see Fig. 4). Thus the final rotation of the $\frac{15}{2}^+$ state in ^{41}Ca was not corrected for any rotation of preceding states, but a larger error was assigned to it.

^{36}Ar is a self-conjugate nucleus. Magnetic moments of such nuclei can be estimated [18] via the isoscalar g factor:

$$g = 0.5 + \Delta g, \quad \Delta g \leq \frac{0.05}{J}. \quad (4)$$

In this context the g factors of the $5^-, 3^-, 2^+$ states excited in the present reaction, Fig. 5, are expected to be almost the same (the small variation arising from the different spins cannot be observed in the present experiment) and equal to ≈ 0.52 .

For levels with (a) meanlives longer than the transit time through gadolinium and (b) equal g factors, measured rotations represent the rotation of each one of the states as if they were directly excited. Thus the measured precisions of the 5^- and 3^- levels, shown in Table II, need not be corrected for any higher cascading state, while the rotation of the 2^+ state, due to its short lifetime, represents mostly the rotation of the 5^- and 3^- states. Finally in Table II the rotations of angular correlations of the three gamma radiations observed in ^{36}Ar were averaged to yield the net precession of the magnetic moment of either of the two states ($5^-, 3^-$).

The g factors of the ^{39}K $\frac{19}{2}^-$ and ^{36}Ar 5^- states were deduced by comparing the measured rotations (Table II) with the rotation and the well-knowing g factor of ^{41}Ca ($g = 0.296 \pm 0.017$) [16,17]. No corrections were applied for the slightly different ion velocities and for the difference in Z. These corrections, of the order of 2.5% for ^{39}K and 5.5% for ^{36}Ar , fall within the statistical errors. The g factor of 0.52 (6) deduced for the $5^-, 4^-$ states of ^{36}Ar is in excellent agreement with the expected value for a self-conjugate nucleus [Eq. (4)], further supporting the calibration based on the magnetic moment of the ^{41}Ca $\frac{15}{2}^+$ state.

V. DISCUSSION

The Transient field: Although determining the parametrization of the transient field was not in our initial intentions, the unexpected high value observed for the strength of the field, experienced by nuclei with $Z \approx 19$ recoiling in gadolinium, give us the impetus to make the following comments.

In Table III, we present the results obtained in the present experiment relevant to the calibration of the transient field. As it can be seen there is a pronounced differentiation between the measured field experienced in

TABLE III. Present transient field data of ions with $Z = 18, 20$ traversing a thin gadolinium foil.

Nucleus J_i^π	$(v/v_0)_{\text{in}}$	$(v/v_0)_{\text{out}}$	$\Delta\theta/g$ (mrad)		R_1^b scaled	R_2^b Rutgers	R_3^b Chalk River		
			measured	scaled ^a					
^{36}Ar $5^-, 3^-$	8.5	4.9	39(4)	26(5)	1.5(3)	1.9(2)	1.5(2)		
	7.6	3.6	39(4)	29(6)	1.3(3)	1.6(2)	1.2(1)		
^{41}Ca $\frac{15}{2}^+$									
R_{mean}							1.4(3)	1.8(2)	1.3(2)

^aScaled value assuming a field linear in velocity and atomic number from data of S and Si in Gd previously published (see text).

^bRatios of the measured rotations to the calculated ones for the various parametrizations of transient field.

gadolinium and that which is known from previous results or from overall parametrizations. In more detail the field shown in column 5 was deduced by extrapolating existing data of S in gadolinium [28] assuming a transient field linear in both the atomic number and the velocity [$B = 1.38(27)kT$ at $v = 8.1v_0$]. Similar results could be obtained by extrapolating data of Si in gadolinium [29]. Subsequently, various parametrizations were considered. Results are shown in columns 6 and 7 adopting the Rutgers parametrization [30]: $B = 96.7Z^{1.1}(v/v_0)^{0.45}M$ and the Chalk River parametrization [31]: $B = 154.65MZ(v/v_0)\exp(-0.135v/v_0)$, where M is the magnetization of the gadolinium foil in T. It should be taken into account, however, that the Rutgers parametrization was done mainly for iron, while for gadolinium it was limited to ions like Se, Sm, and Pt (velocity range $2 \leq v/v_0 \leq 6$). Also the Chalk River parametrization in gadolinium was done for heavy ions, like Gd, Dy, Tm, Pb and in the velocity range $2 \leq v/v_0 \leq 9$.

In columns 8, 9, and 10 ratios of the present measured rotations over those of the scaled field and parametrizations are also shown. From the obtained mean ratios in Table III, 1.4(3), 1.8(2), and 1.3(2) it becomes evident that the field experienced in gadolinium by nuclei around $Z \approx 19$ is bigger than predicted by existing parametrizations. It is thus shown again that precise absolute g factors cannot be deduced by using a general parametrization if this parametrization has not been tested very near the region of interest.

The g factors: Traditionally the determination of magnetic moments has helped to elucidate the structure of states, since they distinguish between single-particle and collective configurations. In particular, nuclei like ^{39}K , almost a doubly magic nucleus, have often provided useful tests for nuclear models.

Several shell-model [32], weak, intermediate, and phonon-particle coupling [8,33] calculations, concerning energy levels and spin assignments, exist in the literature. A detailed discussion of these calculations may be found in Ref. [14]. However, most of them concern the lower energy levels.

For the higher spin states up to 6 MeV, shell-model calculations were performed by Hasper *et al.* [32], considering as active the $2s_{1/2}$, $1d_{3/2}$ orbits and a particle

distribution in the $1f_{7/2}$ and $2p_{3/2}$ orbits. A $\frac{19}{2}$ state is predicted at about 6 MeV, that is, 2 MeV lower than the experimental value. On the other hand, as was already mentioned, the $\frac{19}{2}^-$ state was described by Uhrmacher *et al.* [11] with an $^{36}\text{Ar}(0^+) \oplus f_{7/2}^3$ configuration.

We have performed shell-model calculations in the $d_{3/2}f_{7/2}$ subspace by adjusting only the $f_{7/2}$ binding energy. The limited configuration space is certainly an oversimplification, however, it is not realistically feasible to take into account fully the s - d and f - p shells. The calculated level scheme is presented in Fig. 1 in comparison with the experimental one. As was already discussed, the calculation gives a qualitative idea of the level density for high spin states. Concerning the $\frac{19}{2}^-$ state, the calculation is off in energy only by ≈ 0.3 MeV. This state is described by a 70% $f_{7/2}^3$ configuration while the rest is spread over many hole states. Adopting this configuration a g factor equal to 0.3 was obtained and found to be insensitive to binding energy variations and quenching of the single-particle spin g factor. On the other hand, if we assume a pure $f_{7/2}^3$ configuration and by using the generalized Landé formula and effective g factors from ^{41}Sc and ^{42}Ca for the $\pi f_{7/2}$, $\nu f_{7/2}$ particles, we obtain a g factor of 0.31. Our experimental value, while close to both predictions, cannot differentiate between them but possibly points out the need for more elaborate calculations in an extended subspace.

VI. SUMMARY

It has been shown that in favorable circumstances unambiguous individual g factors can be obtained for picosecond states by using the conventional transient field technique. The high field observed in gadolinium, opens the possibility for performing rather precise measurements in this mass region.

ACKNOWLEDGMENTS

A. Buscemi and R. Zanon are warmly acknowledged for their collaboration in setting up the experiment. One of us (A.A.P.) acknowledges Professor P. Assimakopoulos and Professor N. Benczer-Koller for valuable discussions and for help in preparing this manuscript.

-
- [1] M. Hass, I. Ahmad, R. V. F. Janssens, T. L. Khoo, H. J. Korner, E. F. Moore, F. H. L. Wolfs, N. Benczer-Koller, E. Dafni, K. Beard, U. Garg, P. J. Daly, and M. Piiparinen, *Phys. Rev. C* **39**, 2237 (1989).
 - [2] E. Lubkiewicz, H. Emling, H. Grein, R. Kulesa, R. S. Simon, H. J. Wollersheim, Ch. Ender, J. Gerl, D. Habs, and D. Schwalm, *Z. Phys.* **335**, 369 (1990).
 - [3] D. Ward, H. R. Andrews, A. J. Ferguson, O. Häusser, N. Rud, P. Skensved, J. Keinonen, and P. Taras, *Nucl. Phys.* **A365**, 173 (1981).
 - [4] M. E. Barclay, L. Cleemann, A. V. Ramayya, J. H. Hamilton, C. F. Maguire, W. C. Ma, R. Soundranayagam, K. Zhao, A. Balandia, J. D. Cole, R. B. Piercey, A. Faessler, and S. Kuyucak, *J. Phys. G* **12**, L295 (1986).
 - [5] A. I. Kucharska, J. Billowes, and C. J. Lister, *J. Phys. G* **15**, 1039 (1989).
 - [6] N. Benczer-Koller, M. Hass, and J. Sak, *Annu. Rev. Nucl. Part. Sci.* **30**, 53 (1980).
 - [7] P. D. Bind and B. D. Kern, *Phys. Rev. C* **36**, 873 (1972).
 - [8] J. L. Durell, V. Metag, R. Repnow, A. N. James, J. F. Sharpey-Schafer, and P. von Brentano, *Nucl. Phys.* **A219**, 1 (1974).
 - [9] J. J. Kolata, Ph. Gorodetzky, J. W. Olness, A. R. Poletti, and E. K. Warburton, *Phys. Rev. C* **9**, 953 (1974).
 - [10] J. W. Olness, A. H. Lumpkin, J. J. Kolata, E. K. Warburton, J. S. Kim, and Y. K. Lee, *Phys. Rev. C* **11**, 110 (1975).
 - [11] M. Uhrmacher, J. Dank, N. Wust, K. P. Lieband, and A.

- M. Kleinfeld, *Z. Phys. A* **272**, 403 (1975).
- [12] E. K. Warburton, J. J. Kolata, and J. W. Olness, *Phys. Rev. C* **16**, 2075 (1977).
- [13] H. H. Eggenhuisen, L. P. Ekström, G. A. P. Engelberting, and H. J. M. Aarts, *Nucl. Phys. A* **305**, 245 (1978).
- [14] P. J. Nolan, A. M. Al-Naser, A. H. Behbehani, P. A. Butler, L. L. Green, A. N. James, C. J. Lister, N. R. F. Rammo, J. F. Sharpey-Schafer, and H. M. Sheppard, *J. Phys. G* **7**, 189 (1981).
- [15] F. Pullhofer, *Nucl. Phys. A* **127**, 267 (1977).
- [16] L. E. Young, G. D. Sprouse, and D. Strottman, *Phys. Rev. C* **12**, 1358 (1975).
- [17] M. Uhrmacher, A. Gelberg, F. Brandolini, A. M. Kleinfeld, and K. P. Lieb, *Phys. Lett.* **56B**, 247 (1975).
- [18] P. C. Zalm, J. F. A. van Hienen, and P. W. M. Glaudemans, *Z. Phys. A* **287**, 255 (1978).
- [19] P. Raghavan, *At. Data Nucl. Tables* **42**, 189 (1989).
- [20] F. Brandolini, F. J. Bergmeister, K. P. Lieb, C. Rossi-Alvarez, and M. Uhrmacher, *Hyperfine Interactions* **5**, 275 (1978).
- [21] R. Levy, N. Benczer-Koller, C. Broude, G. Goldring, and K. Hagemeyer, *Z. Phys. A* **301**, 243 (1981).
- [22] D. Bazzacco, F. Brandolini, P. Pavan, C. Rossi-Alvarez, and R. Zannoni, *Nuovo Cimento* **84A**, 106 (1984).
- [23] D. Bazzacco, F. Brandolini, K. Loewenich, P. Pavan, C. Rossi-Alvarez, and R. Zannoni, *Phys. Rev. C* **33**, 1785 (1986).
- [24] H. P. Hellmeister, K. P. Lieb, and W. Muller, *Nucl. Phys. A* **307**, 515 (1978).
- [25] R. Daniels, J. D. Burrows, P. A. Butler, J. R. Cresswell, A. D. Irving, D. J. G. Love, T. P. Morisson, P. J. Nolan, and J. J. F. Sharpey-Schafer, *J. Phys. G* **9**, 947 (1983).
- [26] C. J. Lister, A. J. Brown, L. L. Green, A. N. James, P. J. Nolan, and J. F. Sharpey-Schafer, *J. Phys. G* **2**, 577 (1974).
- [27] K. P. Lieb, M. Uhrmacher, J. Dauk, and A. M. Kleinfeld, *Nucl. Phys. A* **223**, 445 (1974).
- [28] H. J. Simonis, F. Hagelberg, M. Knopp, K. H. Speidel, and W. Karle, *J. Gerber, Z. Phys. D* **7**, 233 (1987).
- [29] D. Bazzacco, F. Brandolini, K. Lowenich, P. Pavan, C. Rossi-Alvarez, M. DePoli, and A. M. Haque, *Z. Phys. D* **14**, 93 (1989).
- [30] N. K. B. Shu, D. Melnik, J. M. Brennan, W. Semmler, and N. Benczer-Koller, *Phys. Rev. C* **21**, 1828 (1980).
- [31] O. Hausser, N. Rud, H. R. Andrews, H. R. Ward, J. Keinonen, and R. Nicole, *Nucl. Phys. A* **412**, 141 (1984).
- [32] H. Hasper, *Phys. Rev. C* **19**, 1482 (1979); S. Maripuu and G. A. Hokken, *Nucl. Phys. A* **141**, 481 (1970); S. T. Hsieh, K. T. Hnopfle, and G. J. Warner, *Nucl. Phys. A* **254**, 141 (1975).
- [33] I. Hamamoto and E. Osnes *Phys. Lett.* **53B**, 129 (1974); S. Wiktor, *ibid.* **40B**, 181 (1972); R. N. Boyd, A. Mignerey, and G. D. Gunn, *Nucl. Phys. A* **281**, 405 (1977); P. R. Goode and L. Zamick, *ibid.* **A129**, 81 (1969); M. J. A. DeVoight, D. Cline and R. N. Horoshko, *Phys. Rev. C* **10**, 1978 (1974); E. Sugarbaker, R. N. Boyd, D. Cline, P. B. Vold, J. R. Lien, and P. R. Goode, *Phys. Rev. C* **19**, 714 (1979).
- [34] C. J. Lister, A. J. Brown, L. L. Green, A. N. James, P. J. Nolan, and J. F. Sharpey-Schafer, *J. Phys. G.* **2**, 577 (1976).
- [35] C. M. Lederer and V. S. Shirley, *Table of Isotopes* (Wiley, New York, 1978).